CHINESE OPTICS LETTERS

Vol. 19, No. 6 | June 2021

Nonlinear Talbot self-healing in periodically poled $LiNbO_3$ crystal [Invited]

Bingxia Wang (王炳霞)[1,2], Shan Liu (刘 山)[3], Tianxiang Xu (徐天翔)[1], Ruwei Zhao (赵茹薇)[1], Peixiang Lu (陆培祥)[2], Wieslaw Krolikowski[3,4], and Yan Sheng (盛 艳)[1,3*]

[1] Laboratory of Infrared Materials and Devices, Research Institute of Advanced Technologies, Ningbo University, Ningbo 315211, China

[2] Wuhan National Laboratory for Optoelectronics and School of Physics, Huazhong University of Science and Technology, Wuhan 430074, China

[3] Laser Physics Center, Research School of Physics, Australian National University, Canberra, ACT 2601, Australia

[4] Science Program, Texas A&M University at Qatar, Doha 23874, Qatar

*Corresponding author: yan.sheng@anu.edu.au

Received March 1, 2021 | Accepted April 8, 2021 | Posted Online April 30, 2021

The nonlinear Talbot effect is a near-field nonlinear diffraction phenomenon in which the self-imaging of periodic objects is formed by the second harmonics of the incident laser beam. We demonstrate the first, to the best of our knowledge, example of nonlinear Talbot self-healing, i.e., the capability of creating defect-free images from faulty nonlinear optical structures. In particular, we employ the tightly focused femtosecond infrared optical pulses to fabricate $LiNbO_3$ nonlinear photonic crystals and show that the defects in the form of the missing points of two-dimensional square and hexagonal periodic structures are restored in the second harmonic images at the first nonlinear Talbot plane. The observed nonlinear Talbot self-healing opens up new possibilities for defect-tolerant optical lithography and printing.

Keywords: nonlinear Talbot effect; nonlinear photonic crystal; periodically poled $LiNbO_3$; second harmonic generation; self-healing.

DOI: 10.3788/COL202119.060011

1. Introduction

Nonlinear photonic crystals (NPCs), also known as periodically poled ferroelectric crystals, have been widely used to extend the wavelength range of coherent light sources[1,2]. The NPC features a spatial modulation of the second-order nonlinear coefficient, such that optical waves with different frequencies can exchange their energies efficiently via the so-called quasi-phase matching[3]. So far, the NPCs have been generalized from simple one-dimensional (1D) periodic modulation[4] to two-dimensional (2D) quasi-periodic[5,6], short-range ordered[7,8], and disordered modulations[9], as well as three-dimensional (3D) periodic modulation[10–12], enabling multi-channel frequency conversion processes with various spatial and spectral resonances. The 2D and 3D NPCs constitute an ideal platform to study new mechanisms and properties of three-wave interactions. For instance, they have been used for observing different kinds of conical emissions of second harmonics (SHs) via the scattered fundamental beam[13], the nonlinear Raman–Nath diffraction[14], and the Čerenkov phase matching[15], respectively. The recent breakthroughs of 3D nonlinearity engineering techniques using femtosecond laser pulses[10,11,16] are opening up new prospects of NPCs in special light generation, nonlinear photonic integration, and high-dimensional optical quantum technologies[17–24].

Nonlinear Talbot self-imaging belongs to one of the most intriguing functionalities of NPCs. The original Talbot effect[25,26], introduced in linear optics, represents self-imaging of a periodic refractive-index pattern (grating) when illuminated by a light beam. The self-imaging and replication of the original refractive-index pattern take place at certain imaging planes in the near field. Analogously, if the medium has a periodicity in its second-order nonlinear susceptibility, the SH waves of the incident laser are diffracted [Fig. 1(a)], and self-imaging can also take place in the SH (frequency 2ω) instead of the incident fundamental beam (ω). This effect is called nonlinear Talbot self-imaging. Since the first, to the best of our knowledge, experimental demonstration in 2010[27], the nonlinear Talbot effect has been observed in NPCs of various structures, such as 1D periodic, as well as 2D square and hexagonal lattices[28–30]. The effect was studied not only at integer nonlinear Talbot planes, but also at fractional planes to fully reveal the evolution of SH waves in the near field[31,32].

One useful characteristic of the Talbot effect is its capability to produce defect-free images from imperfect structures, i.e., the

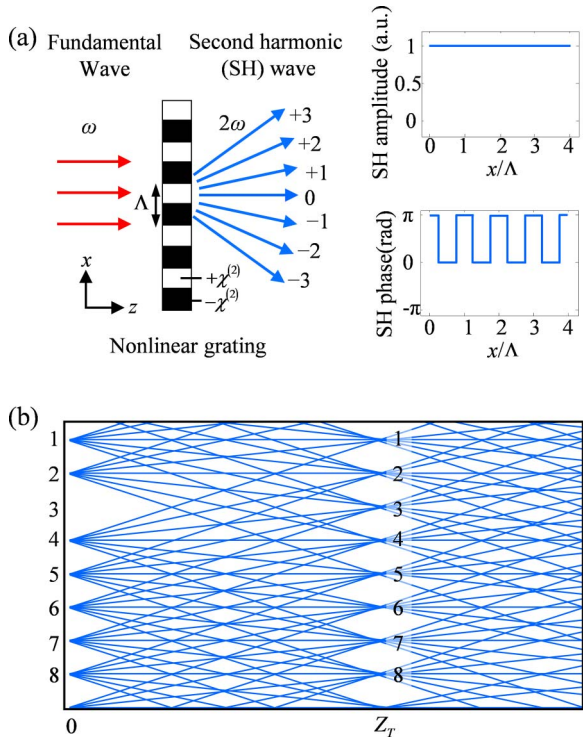

Fig. 1. (a) SH diffraction from a nonlinear $\chi^{(2)}$ grating. The grating has a periodic variation of the sign of the second-order nonlinear coefficient $\chi^{(2)}$, which can generate SH waves with uniform amplitude but periodic phase difference of π. (b) Illustrating Talbot self-healing, where the initially missing point (#3) is restored in the first Talbot image plane.

property known as self-healing. As shown in Fig. 1(b), a defective grating with one missing element can be self-imaged without an apparent defect[33]. While such capability of image restoration has been well known in the linear Talbot effect, it has never been studied in the scheme of nonlinear optics. The nonlinear Talbot effect has an advantage over its linear analogue because its spatial resolution in imaging is improved by a factor of two thanks to frequency doubling. Hence, it may be more useful for applications that require defect-tolerant properties such as the defect-free lithography for nanoscale printing[34].

In this Letter, we use the femtosecond laser poling technique[16] to fabricate $LiNbO_3$ NPCs and demonstrate nonlinear Talbot self-healing in experiments. Instead of producing a perfect periodic structure, we randomly remove a few lattice points from the 2D square and hexagonal lattices. The near-field nonlinear diffraction experiments show that the missing points are restored in nonlinear Talbot self-images.

2. Experiments

To fabricate the NPCs, we employ tightly focused femtosecond infrared optical pulses to invert ferroelectric domains in a z-cut congruent $LiNbO_3$ crystal. The sizes of the crystal are 5 mm × 5 mm × 0.5 mm in length, width, and thickness, respectively. The crystal was mounted on a translational stage that can be

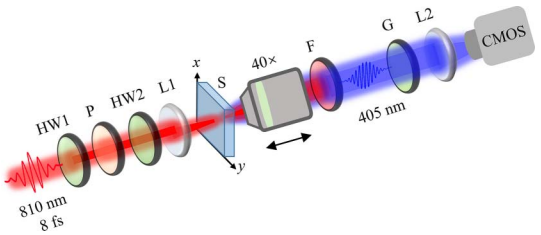

Fig. 2. Experimental setup for nonlinear Talbot self-healing. HW, half-wave plate; P, polarizer; L, lens; S, nonlinear photonic sample; F, short-band-pass filter; G, Glan prism; CMOS, CMOS camera.

accurately positioned in three orthogonal directions. The infrared pulses (150 fs, 800 nm, Mira Coherent) were tightly focused using an objective lens (NA = 0.65) and incident normally to the surface of the crystal. The beam was initially focused on the front ($-z$) surface of the crystal. Then, the sample was translated along the z direction so that the position of the focal region moved throughout the sample to induce ferroelectric domain inversion. After this process, the laser beam was blocked by an automatic shutter, and the sample moved to the next region of domain inversion. In this way, nonlinear photonic structures with square and hexagonal lattices were fabricated. Instead of perfectly periodic structures, some of lattice points were missing on purpose to show nonlinear Talbot self-healing. It should be noted that the optically induced inverted domains did not penetrate through the whole thickness of the $LiNbO_3$ crystal. The average length of these domains is about 20 μm. Their diameters gradually decrease with the thickness, which may slightly affect the overall quality of the nonlinear Talbot imaging.

The setup of the nonlinear Talbot experiment is schematically shown in Fig. 2. A mode-locked Ti:sapphire femtosecond laser (Vitara Coherent) operating at a wavelength of 810 nm is used as the fundamental light source. The pulse width is 8 fs with a repetition rate of 80 MHz. The average power of the fundamental beam was controlled by the combination of a half-wave plate (HW1) and a polarizer (P). Then, another half-wave plate (HW2) was used to control the polarization state. Lens L1 (focal length $f = 5$ cm) was used to focus the y-polarized fundamental beam into the sample (S) with a spot size of ~80 μm, which propagates along the z axis of the crystal. After being collected by a 40× microscope objective and filtering out the fundamental beam by a short-band-pass filter (F), the emitted y-polarized SH was extracted by a Glan prism (G). Since $LiNbO_3$ crystal has a space group of 3 m (C_{3v}), only the d_{22} component contributes to the SHG in our experimental configuration. Finally, the SH was collected by the lens L2 (focal length $f = 10$ cm) and then recorded by CMOS camera (Prime 95B, Phitimetrics). The microscope objective (40×) is mounted on a z-translation stage such that the SH patterns can be recorded at different imaging planes.

3. Results and Discussion

The experimental results of the nonlinear Talbot effect in the square lattice are shown in Fig. 3. As a reference, the nonlinear

Čerenkov microscopic image[35] of the fabricated structure is shown in Fig. 3(a). The period of the square lattice is 5 μm. Some lattice points are missing and marked by the yellow squares in the figure. We chose the patterns exhibiting at the output surface of the crystal as the object, which is shown in Fig. 3(b). This image agrees well with the nonlinear Čerenkov image, with the originally missing points clearly visible. The SH image recorded at the first nonlinear Talbot plane is displayed in Fig. 3(c). It is interesting to see that the missing lattice points are all restored in this image, demonstrating the self-healing property of the nonlinear Talbot effect. According to our measurement, the first nonlinear Talbot plane is located at a distance of $Z_T = 120\,\mu m$ away from the sample's output surface, agreeing well with the theoretical prediction of $Z_T = 4a^2/\lambda = 123.46\,\mu m$[27], where $a = 5\,\mu m$ is the period of the square lattice, and $\lambda = 0.81\,\mu m$ is the fundamental wavelength.

The experiment results of the hexagonally poled NPC are shown in Fig. 4. Nonlinear Talbot self-healing was observed, with the introduced structure defects restored in the first SH Talbot plane again. The SH Talbot distance depends on the symmetries of the periodic lattice. For a 2D hexagonal lattice, the nonlinear Talbot distance $Z_T = 3a^2/\lambda$[31]. Taking the lattice period $a = 5\,\mu m$, the theoretical nonlinear Talbot distance is $Z_T = 92.59\,\mu m$. In experiment, the measured distance is $Z_T = 95\,\mu m$, agreeing well with the calculation.

It is worth noting that nonlinear Talbot self-imaging and self-healing are strongly dependent on the periodicity of the sample. Structural defects can be restored only when they are not severe enough to destroy the structure periodicity. For example, an

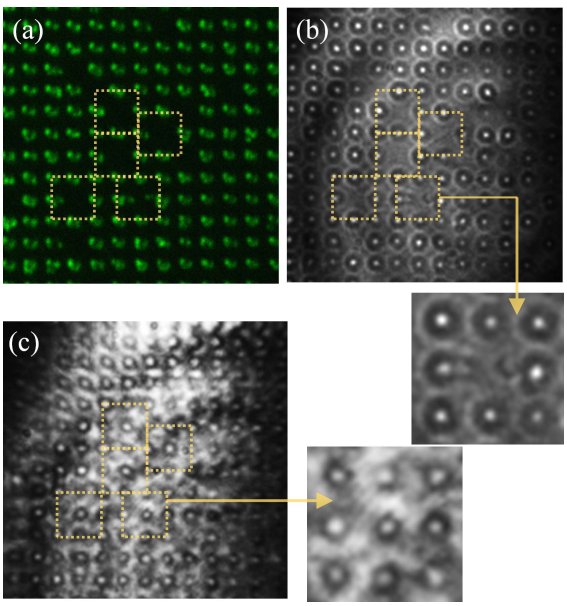

Fig. 3. (a) Čerenkov SH microscopic image of the fabricated NPCs with a square lattice. Several lattice points are missing on purpose to serve as the structural defects (marked by the yellow squares). (b) The ferroelectric domain structure imaged on the output surface of the NPC. (c) The SH self-image at the first nonlinear Talbot plane. The missing lattice points are all restored, indicating the nonlinear Talbot self-healing.

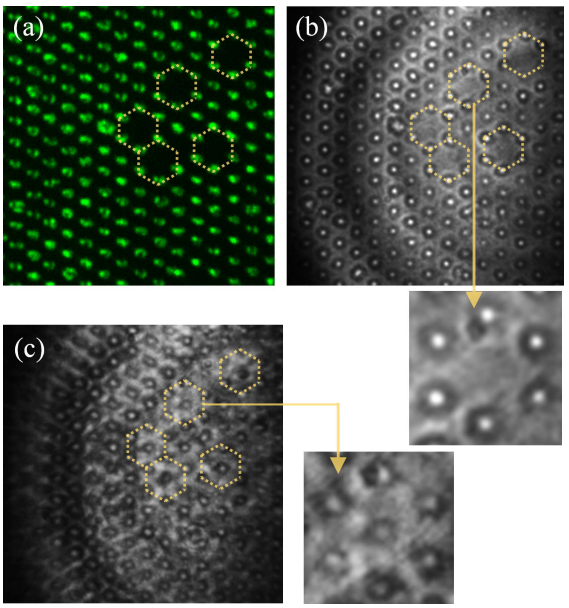

Fig. 4. (a) Čerenkov SH microscopic image of the hexagonally poled $LiNbO_3$ NPCs. The designed defects are several missing lattice points located randomly throughout the sample (marked by the yellow hexagons). (b) The ferroelectric domain structure imaged on the output surface of the NPC. (c) The SH self-image at the first nonlinear Talbot plane, with the missing points being restored.

NPC with a sunflower seed pattern was also tested in experiments. The sunflower spiral has no periodicity in its structure [Figs. 5(a) and 5(b)]. Therefore, we did not observe the nonlinear Talbot self-healing with this structure. In experiment, the SH near-field diffraction from the sunflower pattern led to only

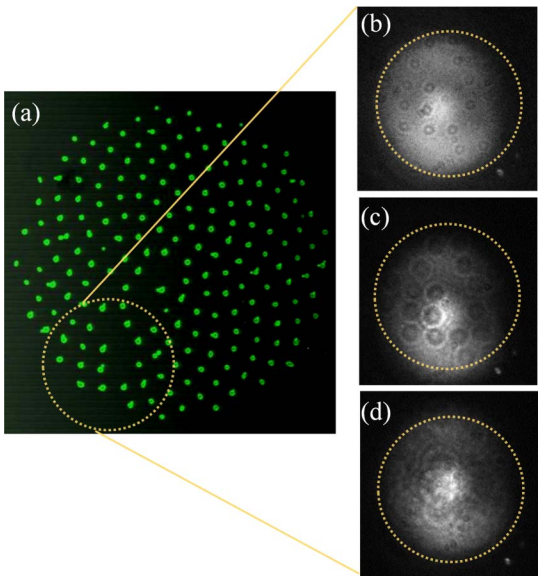

Fig. 5. (a) Čerenkov SH microscopic image of the $LiNbO_3$ NPC with sunflower seed pattern. (b) The ferroelectric domain structure imaged on the output surface of the crystal. (c), (d) The SH near-field diffraction patterns imaged at distances of 20 μm and 50 μm from the sunflower pattern.

blurred images, which got even worse with the increasing imaging distance, as shown in Figs. 5(c) and 5(d).

4. Conclusion

In summary, we have employed tightly focused infrared femtosecond laser pulses to fabricate the $LiNbO_3$ NPCs with square and hexagonal lattices. The structure defects of randomly missing lattice points that are intentionally introduced are well restored in the SH Talbot self-images. Nonlinear Talbot self-healing offers a way to construct defect-tolerant devices, which are highly desirable in applications like optical lithography and nanoscale printing. It works perfectly with periodic $\chi^{(2)}$ structures, but is incapable of dealing with disordered patterns. The resolution of nonlinear Talbot imaging is defined by the diffraction limit at the SH frequency. Our study also indicates that nonlinear Talbot self-healing has to be taken into account when using it to diagnose the structures of NPCs.

Acknowledgement

This work was supported by the National Natural Science Foundation of China (Nos. 61905124, 11974196, and 61905125), the Australian Research Council (No. DP19010774), the Qatar National Research Fund (No. NPRP 12S-0205-190047), the Yongjiang Scholar Foundation of Ningbo, and the K. C. Wong Magna Fund of Ningbo University.

References

1. V. Berger, "Nonlinear photonic crystals," Phys. Rev. Lett. **81**, 4136 (1998).
2. A. Arie and N. Voloch, "Periodic, quasi-periodic, and random quadratic nonlinear photonic crystals," Laser Photon. Rev. **4**, 355 (2010).
3. J. A. Armstrong, N. Bloembergen, J. Ducuing, and P. S. Pershan, "Interactions between light waves in a nonlinear dielectric," Phys. Rev. **127**, 1918 (1962).
4. M. M. Fejer, D. H. Jundt, R. L. Byer, and G. A. Magel, "Quasi-phase-matched second harmonic generation: tuning and tolerances," IEEE J. Quantum Electron. **28**, 2631 (1992).
5. Y. Sheng, J. Dou, B. Cheng, and D. Zhang, "Effective generation of red-green-blue laser in a two-dimensional decagonal photonic superlattice," Appl. Phys. B **87**, 603 (2007).
6. R. Lifshitz, A. Arie, and A. Bahabad, "Photonic quasicrystals for nonlinear optical frequency conversion," Phys. Rev. Lett. **95**, 133901 (2005).
7. Y. Sheng, J. Dou, B. Ma, B. Cheng, and D. Zhang, "Broadband efficient second harmonic generation in media with a short-range order," Appl. Phys. Lett. **91**, 011101 (2007).
8. Y. Sheng, D. Ma, M. Ren, W. Chai, Z. Li, K. Koynov, and W. Krolikowski, "Broadband second harmonic generation in one-dimensional randomized nonlinear photonic crystal," Appl. Phys. Lett. **99**, 031108 (2011).
9. B. Wang, K. Switowski, C. Cojocaru, V. Roppo, Y. Sheng, M. Scalora, J. Kisielewski, D. Pawlak, R. Vilaseca, H. Akhouayri, W. Krolikowski, and J. Trull, "Comparative analysis of ferroelectric domain statistics via nonlinear diffraction in random nonlinear materials," Opt. Express **26**, 1083 (2018).
10. T. Xu, K. Switkowski, X. Chen, S. Liu, K. Koynov, H. Yu, H. Zhang, J. Wang, Y. Sheng, and W. Krolikowski, "Three-dimensional nonlinear photonic crystal in ferroelectric barium calcium titanate," Nat. Photon. **12**, 591 (2018).
11. D. Wei, C. Wang, H. Wang, X. Hu, D. Wei, X. Fang, Y. Zhang, D. Wu, Y. Hu, J. Li, S. Zhu, and M. Xiao, "Experimental demonstration of a three-dimensional lithium niobate nonlinear photonic crystal," Nat. Photon. **12**, 596 (2018).
12. Y. Zhang, Y. Sheng, S. Zhu, M. Xiao, and W. Krolikowski, "Nonlinear photonic crystals: from 2D to 3D," Optica **8**, 372 (2021).
13. P. Xu, S. H. Ji, S. N. Zhu, X. Q. Yu, J. Sun, H. T. Wang, J. L. He, Y. Y. Zhu, and N. B. Ming, "Conical second harmonic generation in a two-dimensional $\chi^{(2)}$ photonic crystal: a hexagonally poled $LiTaO_3$ crystal," Phys. Rev. Lett. **93**, 133904 (2004).
14. S. M. Saltiel, D. N. Neshev, R. Fischer, W. Krolikowski, A. Arie, and Y. S. Kivshar, "Generation of second-harmonic conical waves via nonlinear Bragg diffraction," Phys. Rev. Lett. **100**, 103902 (2008).
15. Y. Sheng, S. M. Saltiel, N. Voloch-Bloch, D. N. Neshev, W. Krolikowski, A. Arie, K. Koynov, and Y. S. Kivshar, "Cerenkov-type second-harmonic generation in two-dimensional nonlinear photonic structures," IEEE J. Quantum Electron. **45**, 1465 (2009).
16. X. Chen, P. Karpinski, V. Shvedov, K. Koynov, B. Wang, J. Trull, C. Cojocaru, W. Krolikowski, and Y. Sheng, "Ferroelectric domain engineering by focused infrared femtosecond pulses," Appl. Phys. Lett. **107**, 141102 (2015).
17. S. Liu, K. Switkowski, C. Xu, J. Tian, B. Wang, P. Lu, W. Krolikowski, and Y. Sheng, "Nonlinear wavefront shaping with optically induced three-dimensional nonlinear photonic crystals," Nat. Commun. **10**, 3208 (2019).
18. D. Wei, C. Wang, X. Xu, H. Wang, Y. Hu, P. Chen, J. Li, Y. Zhu, C. Xin, X. Hu, Y. Zhang, D. Wu, J. Chu, S. Zhu, and M. Xiao, "Efficient nonlinear beam shaping in three-dimensional lithium niobate nonlinear photonic crystals," Nat. Commun. **10**, 4193 (2019).
19. B. Zhu, H. Liu, Y. Liu, X. Yan, Y. Chen, and X. Chen, "Second-harmonic computer-generated holographic imaging through monolithic lithium niobate crystal by femtosecond laser micromachining," Opt. Lett. **45**, 4132 (2020).
20. S. Liu, L. M. Mazur, W. Krolikowski, and Y. Sheng, "Nonlinear volume holography in 3D nonlinear photonic crystals," Laser Photon. Rev. **14**, 2000224 (2020).
21. S. Keren-Zur and T. Ellenbogen, "A new dimension for nonlinear photonic crystals," Nat. Photon. **12**, 575 (2018).
22. J. Imbrock, L. Wesemann, S. Kroesen, M. Ayoub, and C. Denz, "Waveguide-integrated three-dimensional quasi-phase-matching structures," Optica **7**, 28 (2020).
23. G. Hu, X. Hong, K. Wang, J. Wu, H.-X. Xu, W. Zhao, W. Liu, S. Zhang, F. Garcia-Vidal, B. Wang, P. Lu, and C.-W. Qiu, "Coherent steering of nonlinear chiral valley photons with a synthetic Au–WS_2 metasurface," Nat. Photon. **13**, 467 (2019).
24. B. Wang, X. Hong, K. Wang, X. Chen, S. Liu, W. Krolikowski, P. Lu, and Y. Sheng, "Nonlinear detour phase holography," Nanoscale **13**, 2693 (2021).
25. H. F. Talbot, "Facts relating to optical science," Philos. Mag. **9**, 401 (1836).
26. L. Rayleigh, "On the manufacture and theory of diffraction grating," Philos. Mag. **11**, 196 (1881).
27. Y. Zhang, J. Wen, S. N. Zhu, and M. Xiao, "Nonlinear Talbot effect," Phys. Rev. Lett. **104**, 183901 (2010).
28. J. Wen, Y. Zhang, and M. Xiao, "The Talbot effect: recent advances in classical optics, nonlinear optics, and quantum optics," Adv. Opt. Photon. **5**, 83 (2013).
29. D. Liu, Y. Zhang, J. Wen, Z. Chen, D. Wei, X. Hu, G. Zhao, S. N. Zhu, and M. Xiao, "Diffraction interference induced superfocusing in nonlinear Talbot effect," Sci. Rep. **4**, 6134 (2014).
30. X. Zhao, Y. Zheng, H. Ren, N. An, and X. Chen, "Cherenkov second-harmonic Talbot effect in one-dimension nonlinear photonic crystal," Opt. Lett. **39**, 5885 (2014).
31. Z. Chen, D. Liu, Y. Zhang, J. Wen, S. N. Zhu, and M. Xiao, "Fractional second-harmonic Talbot effect," Opt. Lett. **37**, 689 (2012).
32. L. Li, H. Liu, and X. Chen, "Dynamic manipulation of nonlinear Talbot effect with structured light," Opt. Lett. **46**, 1281 (2021).
33. A. Bakman, S. Fishman, M. Fink, E. Fort, and S. Wildeman, "Observation of the Talbot effect with water waves," Am. J. Phys. **87**, 38 (2019).
34. L. Urbanski, A. Isoyan, A. Stein, J. J. Rocca, C. S. Menoni, and M. C. Marconi, "Defect-tolerant extreme ultraviolet nanoscale printing," Opt. Lett. **37**, 3633 (2012).
35. Y. Sheng, A. Best, H. J. Butt, W. Krolikowski, A. Arie, and K. Koynov, "Three-dimensional ferroelectric domain visualization by Čerenkov-type second harmonic generation," Opt. Express **18**, 16539 (2010).